Wind Convergence Observed by QuikSCAT

W. Timothy Liu, Xiaosu Xie, Hua Hu and Wenqing Tang
Jet Propulsion Laboratory, California Institute of Technology

1. Introduction

The National Aeronautics and Space Administration launched a microwave scatterometer QuikSCAT in July 1999. It is providing daily coverage of surface wind speed and direction over 93% of the global ocean, under clear and cloudy conditions, day and night. The high accuracy and resolution made it possible to compute derivative quantities, such as atmospheric wind convergence, which reveal details of the atmospheric processes [Liu, 2002].

2. Interplay Between Wind and Rain in Tropical Cyclones

Scatterometer data have been widely used by marine weather and hurricane centers in analyzing and predicting marine storms. The increasing spatial resolution of scatterometer data provides increasing detailed descriptions of small and intense weather systems, like tropical cyclones [Liu et al. 2000]. Fig. 1 shows that the 12.5-km spatial resolution allows the delineation of surface wind convergence associated with the multiple rainbands of Hurricane Floyd. The winds from the Eta model are not even close to being able to resolve such rain bands. Eta is a regional NWP model producing operational wind products with the highest available spatial resolution (40-km).

Wind, the dynamic parameter, and rain, the hydrologic (latent heat) parameter, are related by the conservation principle. The influence of the ocean surface winds is not confined to the surface, but instead is felt throughout the atmospheric column. The vertical velocity in pressure coordinate ω, at a certain level p, depends on the horizontal wind velocity u at that level and all levels below it, as defined in the equations in Fig. 2. The surface wind affects ω at all levels, and ω affects the 'apparent moisture sink' [Yanai et al., 1973] Q at each level. Q is the difference between condensation c and evaporation e, per unit mass of air. The vertical integration of Q gives the fresh water flux (F), or hydrologic forcing, at the surface. The profile of Q is conventionally expressed as the profile of diabatic heating rate per unit mass of air, H. In the four equations in Fig. 2, q is the specific humidity, t is the time, g is acceleration due to gravity, c_p is the isobaric

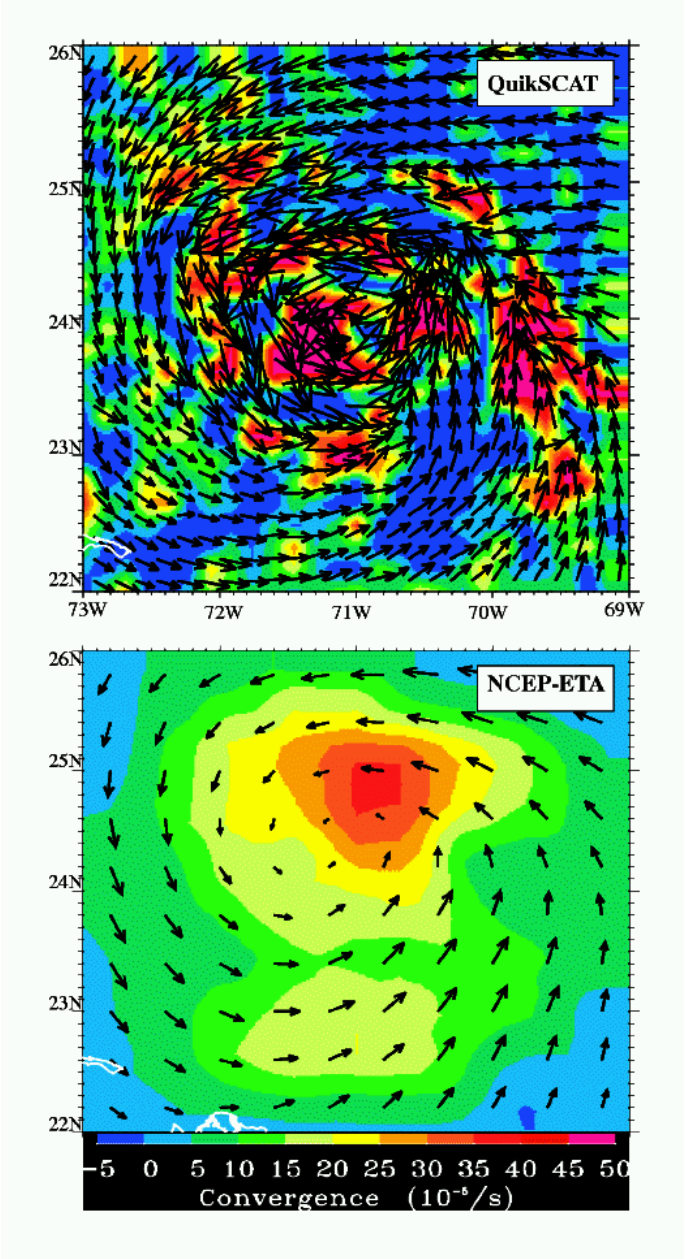

Fig. 1 Hurricane Floyd on 13 September 1999. Black arrows representing wind vectors are superimposed on color image of wind convergence, derived from QuikSCAT (upper), and from Eta model (lower)

Interplay Between Wind and Rain Observed in Hurricane Floyd

$$F = P - E = \frac{1}{g}\int_0^{p_s} Q\,dp$$

$$Q = -\left(\frac{\partial q}{\partial t} + \vec{u} \bullet \nabla_h q + \omega \frac{\partial q}{\partial p}\right) = c - e$$

$$\omega_p = -\int_{p_s}^{p} \nabla_h \bullet \vec{u}\, dp$$

$$H = LQ / c_p$$

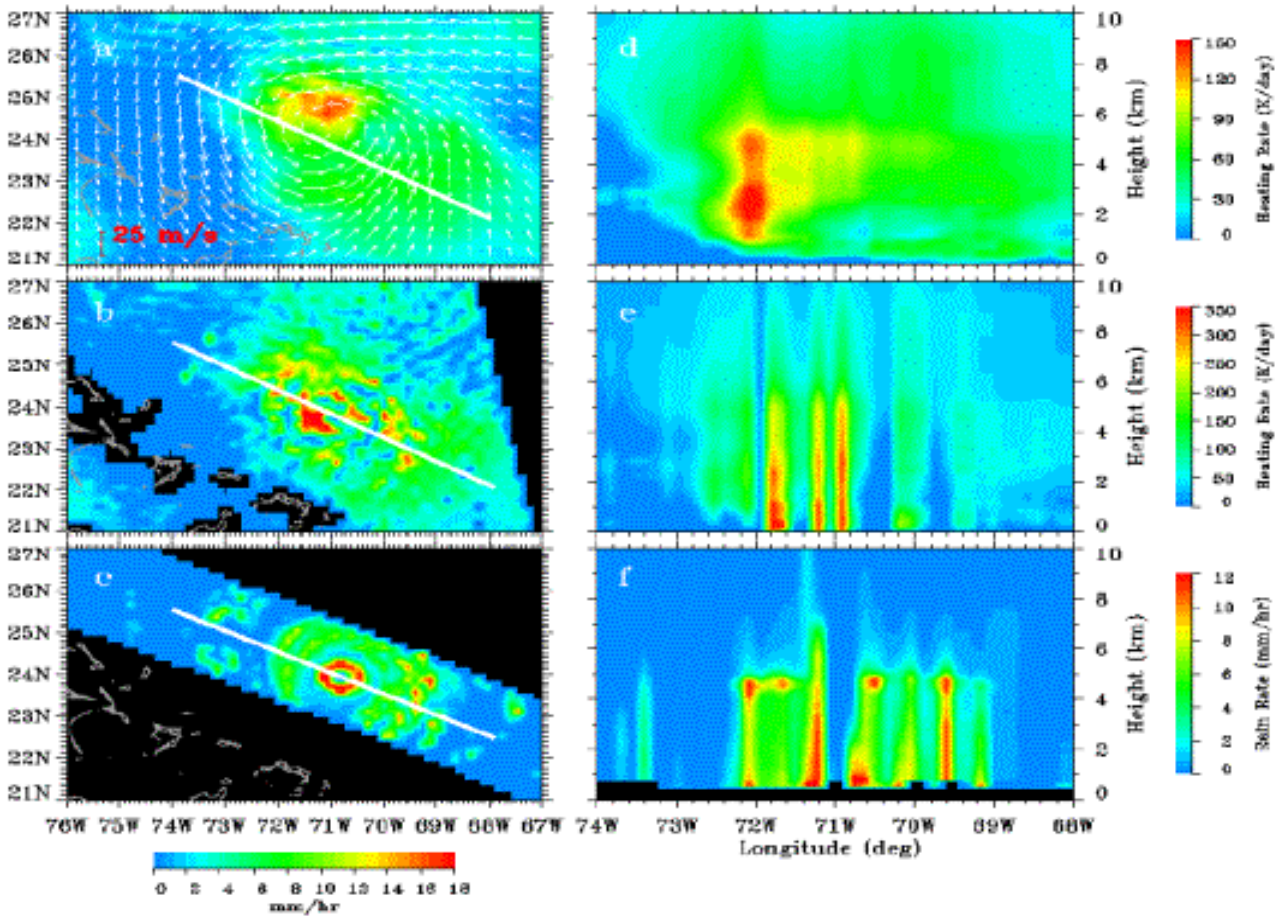

Fig. 2 Hurricane Floyd, as revealed by Eta output, interpolated to 10:48 UT, with white arrows representing winds at 1000 mb and the color image presenting F (upper left); as F computed by replacing the surface wind divergence of Eta output with QuikSCAT data measured at 10:48 UT (center left); as surface rainfall estimated from TRMM PR observations at 9:30 UT (lower left). Vertical profiles of heating and rain rates along the white lines in panels on the left are shown in panels on the right.

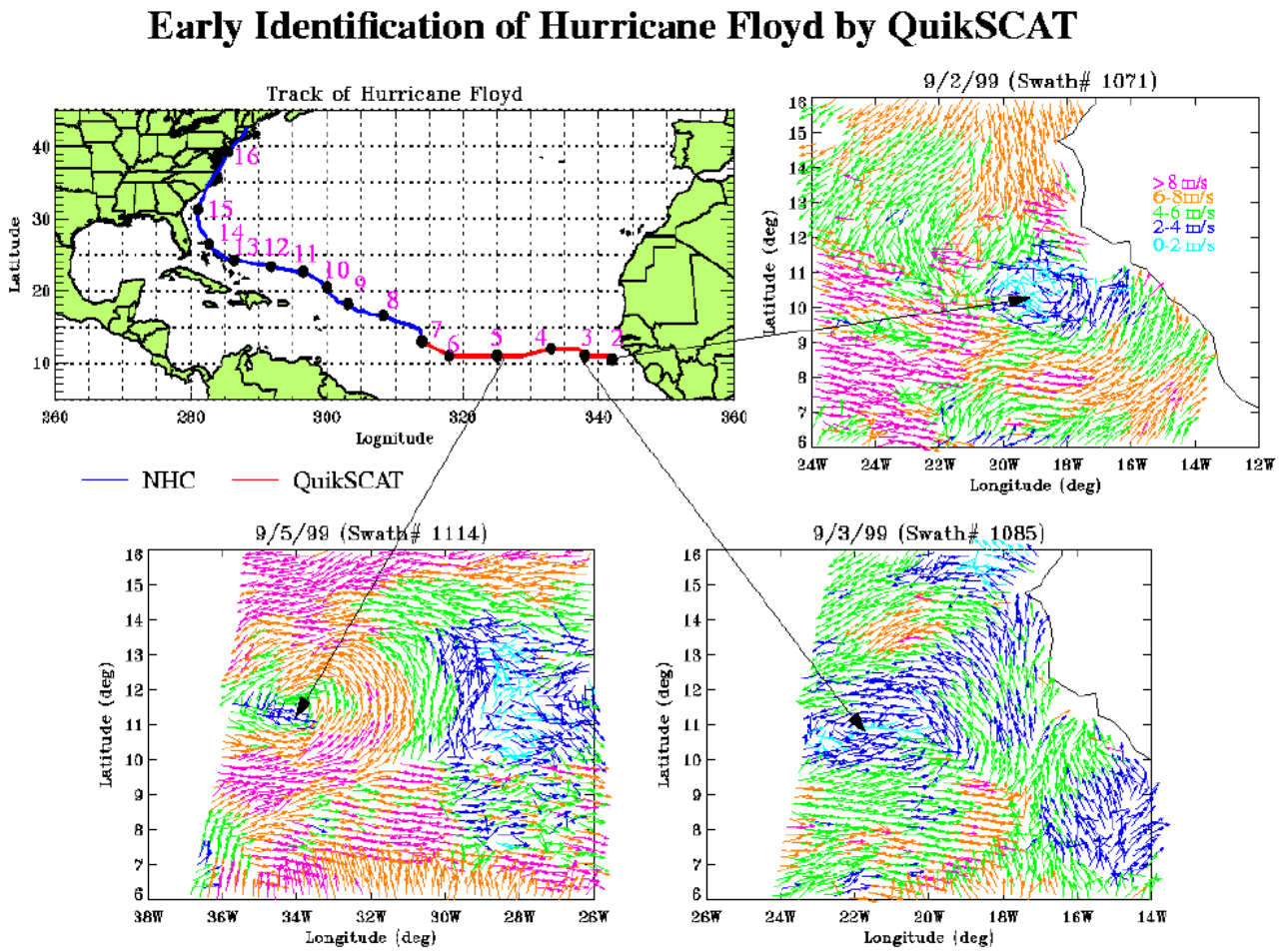

Fig. 3 Track of Hurricane Floyd issued by the National Hurricane Center and revealed by QuikSCAT

Specific heat, L is the latent heat of vaporization, E and P are the evaporation precipitation at the surface. The estimation of F and H should be dependent on the accuracy of surface wind divergence. Provided that the variation of E is small compared with P, the horizontal pattern of F and vertical pattern of H should be comparable to the surface rain pattern and vertical rain profiles measured by TRMM.

The multiple rainbands of hurricane Floyd were clearly visible in surface rain pattern and rain profiles measured by the precipitation radar (PR) on Tropical Rain Measuring Mission (TRMM) (Fig. 2c & 2f). The eta model with conventional data assimilation cannot produce realistic rain patterns for Hurricane Floyd (Fig, 2a & 2c). By simply replacing the wind divergence between 1000 and 975 mb of the Eta products with the divergence of scatterometer wind in the computation of F, the pattern becomes much more realistic with the appearance of the eye and more than one spiral rain bands (Fig. 2b). Walls of precipitations define the rainbands and locate the eye at 77.1°W (Fig. 2e). The precipitation cut-off at 5 km, indicating freezing level, also agrees with observations by PR. Because Hurricane Floyd moves, model results were linearly interpolated to the time of QuikSCAT overpass at 10:48 UT, with the spatial coordinate moving with the eye of the hurricane.

In 1999, the National Hurricane Center declared Floyd a tropical depression on 7 September east of the West Indies. As shown in Fig. 3, QuikSCAT data were used to track the surface vortex all the way back to the shear zone in the monsoon trough off the African coast on September 2, 1999, almost a week earlier [Liu, 2001]. Cyclogenesis (starting of the hurricane heat engine) requires sufficient inertial stability in the atmosphere, as reflected in a small Rossby radius of deformation, to retain the heat released by cumulus convection. A current theory suggests that the stability is achieved by mid-level vortex merging [Ritchie et al., 2002]. After merging, the resultant mid-level vortex strengthens and thickens to reach the surface. The surface circulation, in turn, will feed moisture and ocean energy into the cyclone. In the early stages, the scattered cloud patterns revealed by weather satellite (Fig. 4) do not appears to be related to surface vortex and cannot dispel the doubt on whether surface vortex plays any role in the mid-level vortices merging that happens much later in the genesis of Floyd. A careful examination of the distribution of surface wind convergence, however, show that, even at the early stages, the cloud patterns (mid-level vorticity) are collocated with surface wind convergence associated with the surface wind vortex (Fig. 4). The high resolution surface wind vectors from QuikSCAT provide a good opportunity for a more objective examination of the relation between surface circulation and mid-level vorticity, in the genesis of hurricanes.

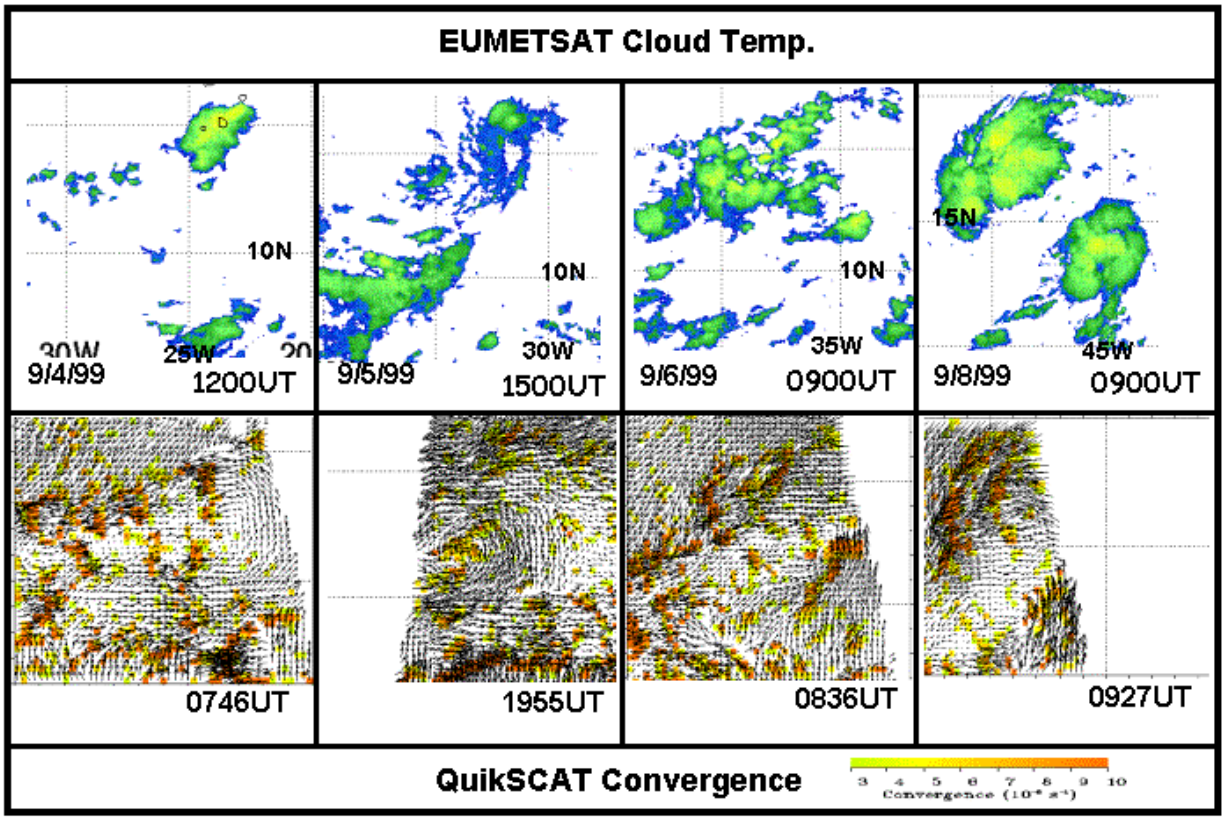

Fig.4 Comparison of EUMETSAT infrared images (top) and QuikSCAT surface wind vectors and convergence for the vortex that evolved into Hurricane Floyd.

3. Intertropical Convergence Zones

The Intertropical Convergence Zones (ITCZ) north of the equator in the eastern Pacific and the Atlantic Oceans and their seasonal meridional migrations were well observed from space, mostly through cloudiness and rainfall in the past. Despite many studies, the existences and seasonality of the ITCZ south of the equator is still controversial. By

definition, ITCZ should be examined through surface wind convergence, but surface wind convergence are largely not available in the past because of the poor resolution of wind maps computed from routine ship reports. Using QuikSCAT winds, the weaker convergence zones south of the equator were revealed in the eastern Pacific and across the entire Atlantic most of the time during the annual cycle. Two different mechanisms which distinguish the formation of stronger from the weaker ITCZ were revealed by the vector winds from QuikSCAT and the sea surface temperature (SST) from the microwave imager on TRMM [Liu and Xie, 2002].

The surface wind convergence is defined as

$$C = -(\frac{\partial u}{\partial x} + \frac{\partial v}{\partial y})$$

where u and v are the zonal and meridional components of surface winds. Near the equator, $-\partial u/\partial x$ is much smaller than $-\partial v/\partial y$; wind convergence is dominated by the meridional gradient of the meridional wind component. In the eastern and western Atlantic, Fig. 5a and 5b show that the northern ITCZ, denoted by the high values of C, is collocated approximately with the v=0 line, where the northerly wind meets the southerly winds and v changes sign. This is also the location of the local maxima of SST, in general. In the eastern Atlantic, a weaker ITCZ is present around 5°S, almost all year round, except for the September-October period. In the west Atlantic, the ITCZ splits into north and

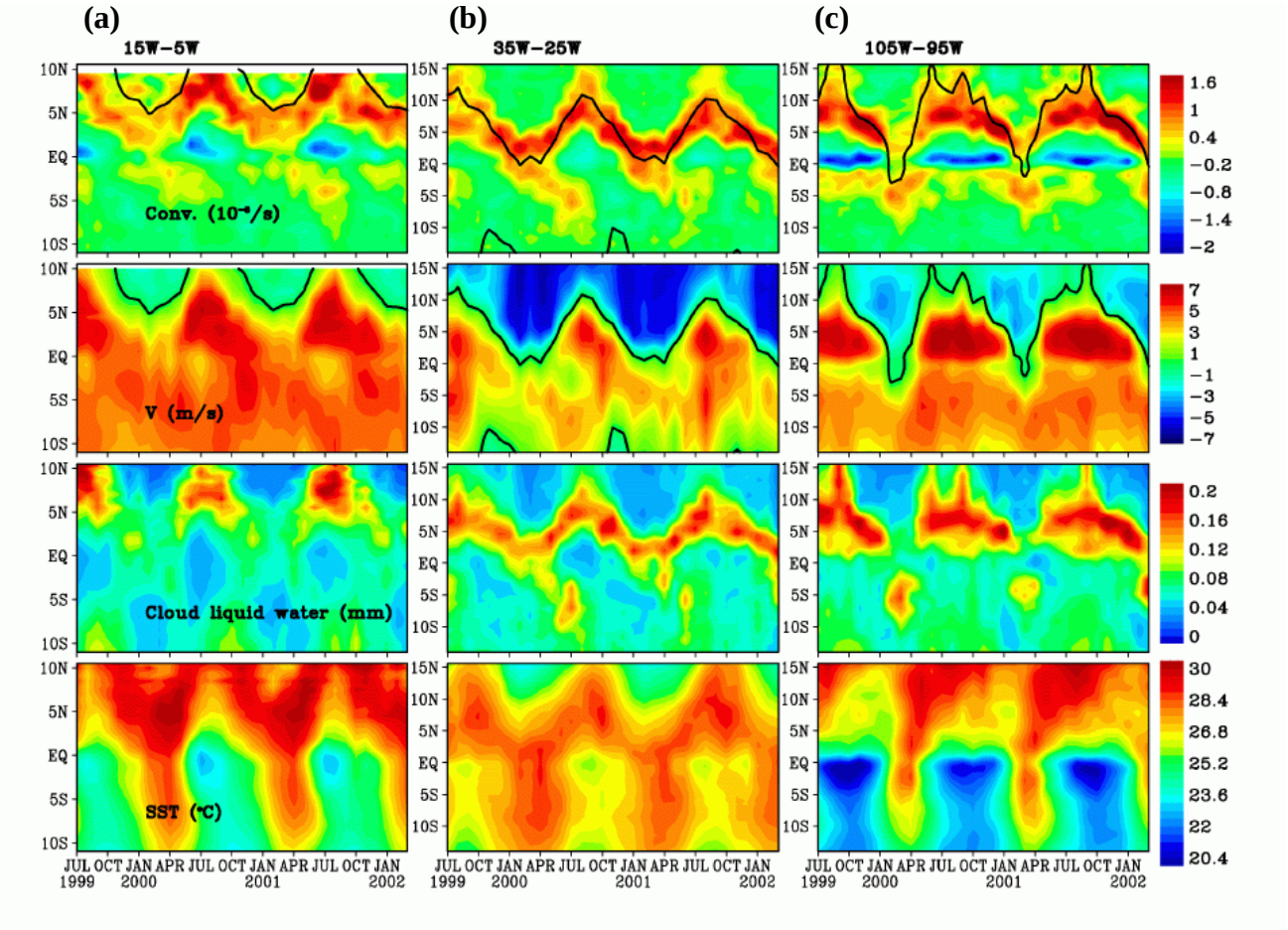

Fig. 5 Latitude-time variations of (from top to bottom) surface wind convergence (10^{-5}/s), meridional wind component (m/s), cloud liquid water (mm), and sea surface temperature (°C), from QuikSCAT and TMI, averaged over (a) 5°W-15°W, (b) 25°W-35°W, and (c) 95°-105°W. On the back line, the meridional wind is zero.

south branches between May and December. The Atlantic, south of the northern ITCZ, is largely dominated by southerly winds, all year round. Because no northerly winds are observed blowing from the equator to the SITCZ, a mechanism different from the one described for the northern ITCZ is needed. There are two scenarios to achieve local maximum of C. High C occurs when v changes from positive to negative, where the southerly trade winds meet the northerly trade winds over the warm water. For the 32 months of QuikSCAT observations, this type of convergence takes place only on one side of the equator, not on both sides. The coexistence of a stronger convergence zone on one side of the equator with a weaker one on the other side cannot be explained with the same mechanism. The second scenario is that local convergence occurs when v decelerates. As the trade winds move from the warmer water with a relatively well-mixed boundary layer towards the cold upwelling water near the equator, vertical mixing is suppressed and wind shear increases. The trade winds decelerate and create a region of convergence just before they reach the cold water. The scenario is similar in the eastern Pacific (Fig. 5c), except that during boreal springs, the northerly trade winds cross the equator and meet the southerly trade winds at the stronger convergence south of the equator.

The QuikSCAT winds are limited to 32 months and are not sufficient to discern interannual variations. Although ocean wind vectors from the ERS scatterometers and from the Special Sensor Microwave Imager [Atlas et al., 1996] do not have the spatial resolution to provide the quality of wind convergence as QuikSCAT, they provide longer time series of data, 1992-2001, and 1987-2001, respectively. The measurements of v by these two sensors are found to exhibit the same characteristics as the QuikSCAT data. For the long time series in the Atlantic, the stronger convergence zone is always in the north and weaker one in south consistent with two mechanisms we postulated. In the eastern Pacific, both sets of data (Fig. 6) show weak surface winds are found blowing both northward and southward from the cold equatorial water towards the double ITCZ, in the boreal springs of 1988, 1994, 1996, and 1999, when the distribution of SST is

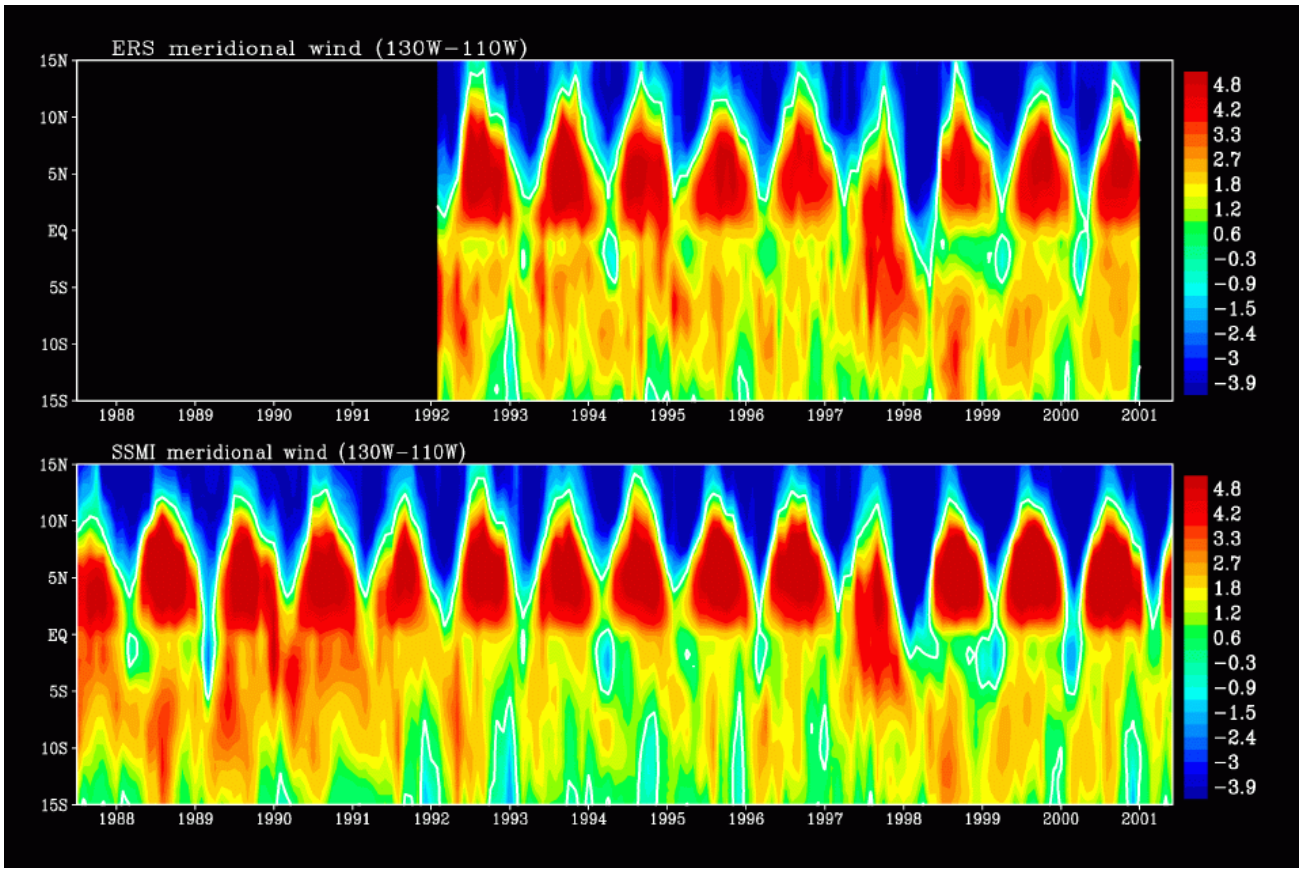

Fig. 6 Latitude-time variations of meridional components of surface wind from ERS scatterometer (upper) and SSM/I (lower) in the eastern tropical Pacific.

more symmetric across the equator. In the boreal springs of 1989, 2000, and 2001, the northeast trades cross the equator and the stronger convergence zone is in the south, as shown by the QuikSCAT data.

4. Wind and Sea Surface Temperature Coupling

This hypothesis of tropical ocean atmosphere coupling through vertical mixing that was used to explain the weaker ITCZ was first used by Xie et al. [1998] to explain the coherence between SST and surface wind in the tropical instability waves (TIW)-the westward propagating temperature front of the cold tongue. Liu et al. [2000] validated this model with rawinsonde measurements of a research cruise across the TIW, and with the phase difference between the wind components measured by QuikSCAT and SST from TMI. They showed that the wind divergence is in quadrature rather than in phase with SST. The same model was implied in a number of studies of TIW, including Wentz et al. [2000] who tested the model with the boundary parameterization of Liu et al. [1979], and Hashizume et al. [2002] who related boundary layer structure to pressure gradient using rawinsonde soundings.

Similar relation between SST and surface winds appears to be much more prevalent. It was observed in the cold patches left behind typhoon passages [Lin et al., 2002b] and even over Gulf Stream rings [Park and Cornillon, 2002]. Xie et al. [2002] demonstrate similar relation in the Asian marginal seas. The vertical mixing mechanism appears to be applicable over a broad spectrum of temporal and spatial scales over different regions. Wind convergence and the associated vorticity were also observed over a narrow band of warm water and eastward currents, creating a break in the westward trade winds and North Equatorial Current; this break stretches from the Western Pacific to the Hawaiian Islands - the results of positive air-sea coupling [Xie et al., 2002].

Acknowledgments

This study was performed at the Jet Propulsion Laboratory, California Institute of Technology under contract with the National Aeronautics and Space Administration (NASA). It was jointly supported by the Ocean Vector Winds, Physical Oceanography, and Tropical Rain Measuring Mission Programs of NASA. Hal Pierce kindly provided the Eumetsat cloud pictures.

References

Atlas, R., R. Hoffman, S. Bloom, J. Jusem, J. Ardizzone, A Multi-year Global Surface Wind Velocity Data Set Using SSM/I Wind Observations. *Bull. Amer. Meteor. Soc.*, **77**, 869-882, 1996.

Bryan, E., and A. Oort, 1984: Seasonal variation of the global water balance based on aerological data. J. *Geophys. Res*., **89**, 11717-11730.

Hashizume, H., S.-P.Xie, M. Fujiwara, M. Shiotani, T. Watanabe, Y. Tanimoto, W.T. Liu, K. Takeuchi, 2002: Direct observations of atmospheric boundary layer response to slow SST variations over the eastern equatorial Pacific, *J. Climate*, in press.

Liu, W.T., 2001: Wind over troubled water. *Backscatter***, 12**, No. 2, 10-14

Liu, W.T., 2002: Progress in scatterometer application, *J. Oceanogr*., **58**, 121-136.

Liu, W.T. and X. Xie, 2002: Double Intertropical Convergence Zoens – a new look using scatterometer. *Geophys. Res. Lett*., in press.

Liu, W.T., K.B. Katsaros, and J.A. Businger, 1979: Bulk parameterization of air-sea exchanges in heat and water vapor including the molecular constraints at the interface. *J. Atmos. Sci.,* **36,** 1722-1735.

Liu, W.T., H. Hu, and S. Yueh, 2000: Interplay between wind and rain observed in Hurricane Floyd. *Eos, Trans. of AGU*, **81**,253 & 257.

Liu, W.T., X. Xie, P.S. Polito, S. Xie, and H. Hashizume, 2000: Atmosphere manifestation of tropical instability waves observed by QuikSCAT and Tropical Rain Measuring Missions. *Geophys. Res. Lett*., **27**, 2545-2548.

Park, K-A., and P. Cornillon, 2002: Stability-induced modification of sea surface winds over Gulf Stream rings. *Geophys. Res. Lett.*, in press (2002GL014236)

Ritchie, E., J. Simpson, W.T. Liu, C. Veldon, K. Brueske, and J. Halvorsen, 2002: A closer look at hurricane formation and intensification using new technology. *Coping with Hurricanes*. Chapter 12, R. Simpson, M. Garstang, and R. Anthes (eds.), Amer. Geophys. Union, in press.

Wentz, F.J., C. Gentemann, D. Smith, D. Chelton, 2000: Satellite measurements of sea surface temperature through clouds. *Science*, **288**, 847-850.

Xie, S.-P., M. Ishiwatari, H. Hashizume, and K. Takeuchi, 1998: Coupled ocean-atmosphere waves on the equatorial front. *Geophys. Res. Lett.*, 25, 3863-3866.

Xie, S.-P., J. Hafner, Y. Tanimoto, W.T. Liu, H. Tokinaga, and H. Xu, 2002: Bathymetric effect on the winter climate of the Yellow and East China Sea., *Geophys. Res. Lett.*, submitted.

Yanai,M., S. Esbensen, and J.H. Chu, 1973: Determination of bulk properties of tropical cloud clusters in large-scale heat and moisture budgets. *J. Atmos. Sci*., **30**, 611-627.